SPNets: Human-like Navigation Behaviors with Uncertain Goals

Nicholas Sohre
sohre007@umn.edu
University of Minnesota CSE Dept
Minneapolis, Minnesota

Stephen J. Guy
sjguy@umn.edu
University of Minnesota CSE Dept
Minneapolis, Minnesota

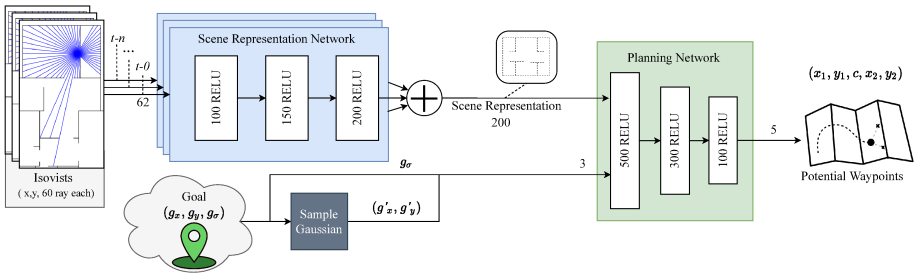

Figure 1: SPNet Network Structure: Isovist feature rays from the path history are transformed by the scene representation network and accumulated into a scene representation. The planning network predicts two potential actions it thinks are likely to lead to efficient paths given the representation, along with a relative confidence between the two choices.

ABSTRACT

Most path planning techniques use exact, global information of the environment to make optimal or near-optimal plans. In contrast, humans navigate using only local information, which they must augment with their understanding of typical building layouts to guess what lies ahead, while integrating what they have seen already to form mental representations of building structure. Here, we propose Scene Planning Networks (SPNets), a neural network based approach for formulating the long-range navigation problem as a series of local decisions similar to what humans face when navigating. Agents navigating using SPNets build additive neural representations of previous observations to understand local obstacle structure, and use a network-based planning approach to plan the next steps towards a fuzzy goal region. Our approach reproduces several important aspects of human behavior that are not captured by either full global planning or simple local heuristics.

CCS CONCEPTS

• **Computing methodologies** → **Real-time simulation**; **Animation**; **Machine learning**; **Planning and scheduling**.

KEYWORDS

Path planning, navigation, character simulation, deep neural networks

MIG '20, October 16–18, 2020, Virtual Event, SC, USA

ACM ISBN 978-1-4503-8171-0/20/10…$15.00
https://doi.org/10.1145/3424636.3426911

ACM Reference Format:
Nicholas Sohre and Stephen J. Guy. 2020. SPNets: Human-like Navigation Behaviors with Uncertain Goals. In *Motion, Interaction and Games (MIG '20), October 16–18, 2020, Virtual Event, SC, USA.* ACM, New York, NY, USA, 11 pages. https://doi.org/10.1145/3424636.3426911

1 INTRODUCTION

The interactive simulation of human motion is important in many scenarios, with applications ranging from video games to building design and smart city planning all benefiting from high-quality human movement and behavior. Recent years have seen many exciting advances centered around developing more human-like approaches in areas such as collision avoidance [Dutra et al. 2017] and character animation [Lee et al. 2019]. However, there has not been similar progress in developing human-like approaches to mid-level task of determining how an agent plans long-term paths through an environment. Here, we work to close that gap by proposing a human-like approach to global navigation planning.

When navigating in new or unfamiliar environments, humans must develop long term navigational plans to reach their goals, while only seeing local information (e.g., doors, walls, and hallways), and are often uncertain about the precise goal locations. Cognitive Science has revealed several key components of human navigation behaviors, such as looking for long goal directed avenues [Bailenson et al. 2000; Lima et al. 2016] and the use of *fuzzy mental maps* to aid in decision making [Epstein et al. 2017; Kaplan et al. 2017]. In this article, we propose the Scene-Planning Network (SPNet) framework. SPNet emulates the human-like approach to global navigation through a custom neural network structure that first builds up an additive representation of the places an agent has explored so far, and then leverages that representation, together with uncertain goal locations, to develop a (stochastic) plan of what next action is likely to make progress toward the goal. Our approach captures several important behaviors that are not possible with

either full global planning or simple local heuristics: SPNet agents will integrate the history of what they have seen to improve their navigation, make different decisions in response to varying levels of certainty with the task at hand, and will stochastically follow a variety paths in situations where multiple different paths to reach the goal are reasonable. Importantly, the training approach used in SPNet reaches human-like performance on these tasks without requiring any human training data, allowing the approach to be easily adopted in a variety of applications.

2 RELATED WORK

Our method draws from research in Computer Graphics, Deep Learning, and Cognitive Science. Here we examine some closely related work from these fields.

2.1 Local & Global Navigation

Previous work in human-like navigation has considered both local and global contexts. Related work in local navigation has focused on realistic behaviors [Kapadia et al. 2015; Karamouzas et al. 2017; McDonnell et al. 2008], often with data-driven [Charalambous and Chrysanthou 2014; Karamouzas et al. 2014; Wang et al. 2016] or geometric [van den Berg et al. 2008] reactive approaches. Others have looked to produce realistic local behaviors by modeling problems similarly to what humans experience [Lee et al. 2019; Ondřej et al. 2010]. Here, we take a similar approach, broadening the scope to considering compelling human-like behavior in the context of global navigation.

Graph search has been used for global navigation in interactive games, VR, and animation to allow virtual characters to plan over a graph-like representation of their environment, producing graph-optimal global routes to their goals, [Botea et al. 2013; van Toll et al. 2016]. Other works have focused on acceleration techniques [Lee and Lawrence 2013], or exploiting heuristics and optimized structures to accelerate the search [Kallmann and Kapadia 2014]. Planners such as Rapidly-exploring Random Trees and its variants [LaValle 1998] use a sampling based approach to build plans in continuous environments under control constraints, while others apply computer vision to directly predict next actions [Rabiee and Biswas 2019], perform waypoint navigation [Bansal et al. 2020], or vision-based navigation [Gupta et al. 2017].

Very related to our work is the area of agent-centered search. Works in this field provide approaches for real-time heuristic search under local information and time constraints. Approaches such as D* Lite [Koenig and Likhachev 2002] and LRTA* [Korf 1990] incrementally learn heuristic information in an online fashion, and extensions focus on improving convergence properties [Hernández and Meseguer 2005], learning speed ([Koenig and Sun 2009; Sturtevant and Bulitko 2011]), and memory efficiency [Bulitko and Björnsson 2009]. LRTS provides a learning framework with a tunable relationship between performance and optimality [Bulitko 2004]. Here, our work will focus on creating human-like behavior (as opposed to guarantees on heuristic admissibility) while allowing the goal to be fuzzy (our agents only have a distribution describing where the goal may be).

2.2 Deep Learning

Deep Learning (DL) techniques have been broadly applied to train large neural networks in many fields [Sze et al. 2017]. Approaches for navigation can either be supervised with known training data (as in [Pfeiffer et al. 2017]), or the network can be trained to optimize path cost using reinforcement learning (as in [Tamar et al. 2016] and [2018]). Deep reinforcement learning (DRL) has recently shown promise for navigation as a fine-tuning final step, as was done in [Pfeiffer et al. 2018] and [Luo et al. 2020]. Very recent work has sought to improve the practicality of DRL navigation by augmenting it with classical, analytical planners([Chaplot et al. 2020]). Neural networks have also proven useful in transforming raw input into rich and meaningful representations [Cai et al. 2019; Doersch 2016]. Additionally, works such as [Peters and O'Sullivan 2002] have used learning techniques to model ways people understanding sensory information. Eslami et al. used an additive representation network to encode virtual scene descriptors that can be used to query views from novel perspectives [Eslami et al. 2018]. A similar cognitive structure has recently be used for efficient robot navigation on a grid [Gupta et al. 2017]. We adapt a similar architecture to build scene representations in a continuous environment.

3 LOCAL-GLOBAL PLANNING

Like humans, SPNet agents are assumed to have only local, limited information about their environment and imprecise knowledge of their long term goals. The agent's task, then, is to integrate its local observations, together with a learned understanding of typical building layouts, to plan efficient paths toward likely goal locations. We assume the agent is updated in real-time following a sense-plan-act loop where it computes its direction of travel frequently based on its history of recent observations.

This section details the underlying problem formulation and path execution strategy of the SPNet framework. In the next section we will introduce a novel network structure which makes the actual predictions of the next optimal step for the agent.

3.1 Problem Formulation

Given a single agent tasked with navigating to given goal whose location is not precisely known, we represent each aspect of the problem as follows:

Agent Representation. The agent is represented by a circle with a radius r large enough to encompass the collision model associated with the agent's animation.

Environment Representation. The agent's environment is defined by a series of line-segments which represent impassible obstacles, and the agent is assumed to be able to move otherwise freely and continuously in $\mathbb{R}^2$. An example map can be seen in Figure 2.

Goal Representation. An agent is not given the exact location of its goal, but rather only a general fuzzy notion of its location. We represent this as 2D Gaussian distribution centered at (μ_x,μ_y), with a standard deviation of σ in each dimension.

Sensing and memory. An agent can only directly observe the portion of line segment obstacle walls which are visible from its current position. In practice, we represent this as a series of i rays

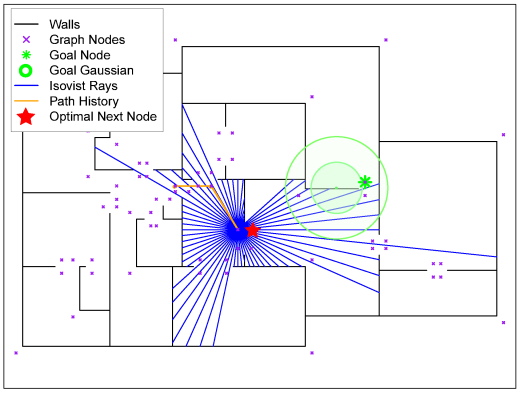

Figure 2: Feature Representation. The goal distribution is shown as 1 and 2 standard deviation rings (σ= 2m).

centered on the agent, whose length is the distance to the wall. Together these rays form a visibility *isovist* from the point of view of the agent. An example isovist can be seen in Figure 2 (blue rays). At any moment, the agent is assumed to have access not only to its current visibility isovist, but also up to the last n isovists it has previously seen. In this way, agents have memory of the past.

For all results, we use i = 60 rays to capture the local visibility isovist. The agent's memory length n is capped at 3 in training, but is allowed to grow to larger values in execution.

3.2 Execution Strategy

The optimal path between any two points in a 2D map can always be found by connecting straight lines between corners or ends of walls [Lozano-Pérez and Wesley 1979]. We refer to any such (potentially optimal) point as a navigation node, and statically compute all such navigation nodes for any map (purple x's in Figure 2). This discretizes the continuous navigation problem without sacrificing any potential path quality by choosing between reachable navigation nodes. We move navigation nodes to be r away from the closest wall to account for the agent's radius.

Our fundamental execution strategy is as follows. Given a set of navigation nodes, a start node, and a goal distribution, our agents utilize a neural-network to select the next navigation node to travel to. At each step, given the current and recent local visibility isovists, the network predicts the next optimal node position. The agent then moves to whichever of the neighboring navigation nodes (e.g., currently visible nodes) is closest to the network's prediction. To guarantee the agent eventually reaches the goal (and avoids infinite travel loops), we introduce a *maxVisitCount* parameter, which specifies the maximum number of times the agent can visit the same node before the node is removed from consideration. A more in-depth description of execution can be found in Appendix A.

4 LEARNED NAVIGATION

SPNet's novel network-based formulation encapsulates both the process of the agent building a mental map of the environment and planning the next best location towards which to move. In this section we both describe the network architecture and discuss the training approach.

4.1 Network Structure

The structure of our prediction network (shown in Figure 1) draws on the idea of mental maps. Rather than taking in a visibility isovist (or series of isovists) and directly predicting the next location, we divide the tasks into separate responsibilities: a Scene Representation Network whose job is to build a representation of map seen so far, and a Planning Network, which takes this representation along with the (fuzzy) goal location and predicts the next step to take. This separation of responsibilities also leads to greater flexibility in how the network is used in execution.

We implement the Scene Representation Network using a three layer neural network (500-300-100 nodes respectively), with a ReLU activation function between each layer. The input of this network is the normalized 60 isovist ray lengths, together with the x and y offset of where the isovist was seen relative to the agent's current position. The output of this network is a 200 valued feature vector which represents the environment. The Scene Representation Network is run once for each isovist in the agent's *path history*, defined as the most recent n isovists (and their offsets) that the agent has seen. The resulting encoding from each isovist are then summed to produce the final 200-dimensional scene representation vector. Critically, this additive representation does not require the agent to use a fixed path history size in execution or training. Summing the Scene Representation Network output over more or fewer previously observed isovists will change the agents behavior in a natural fashion. This behavior tuning is discussed further in Section 5.2.

The Planning Network combines the 200-dimensional scene representation together with the goal region to determine the likely next actions. The goal input is represented as three parameters defining a Gaussian which describes a distribution over possible goal locations. These values are concatenated with the encoding, and the resulting 203 dimensional vector is then passed through another three layer network (100-150-200 nodes respectively), with a ReLU activation function between each layer. The output of this network encodes the next step for the agent to take.

4.2 Navigation Prediction

Rather than producing a single 2D coordinate for the next navigation step, our network outputs a stochastic prediction split over two alternatives: $p_0 = (x_0, y_0)$ and $p_1 = (x_1, y_1)$ represent the probable offsets (relative to the agent) of optimal next navigation nodes, and c ranges continuously from 0 to 1 represent the network's choice between p_0 and p_1 (0 for choice 0, 1 for choice 1).

We train this output using a three-part loss function:

$$\mathrm{L}(p_0, p_1, c, y) = k_m \mathrm{L}_{\min} + k_a \mathrm{L}_{\text{avg}} + k_p \mathrm{L}_{\text{pred}} \tag{1}$$

with p_0, p_1, and c as defined above, y as the true optimal prediction for this scenario, and k_m, k_a, and k_p as tuning parameters that relatively weight the three components of the loss.

Each of the three components of the loss function serves a different purpose. The first term:

$$\mathrm{L}_{\min}(p_0, p_1, y) = \min(s_0 \|p_0 - y\|, s_1 \|p_1 - y\|) \tag{2}$$

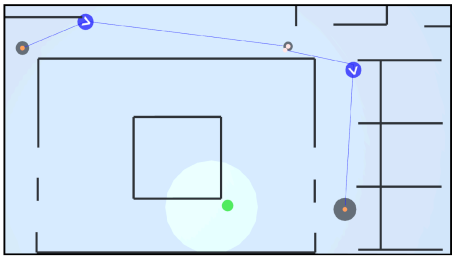

Figure 3: Prediction under Ambiguity. The agent (blue) navigates to its goal (green) from 2 locations in a courtyard-style map. Blue lines terminate at predictions (larger grey circle → more confident prediction). Unambiguous scenarios produce greater confidence in the chosen direction.

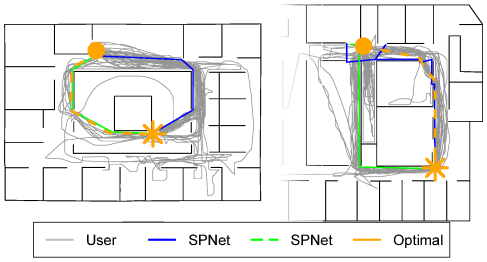

Figure 4: Human-Like Behavior: SPNet produces efficient, human-like paths both for maps on which it was trained (left), and maps not seen in training (right).

measures how close the better of the two predictions is to the optimal next node. The s_i terms, computed as $s_i = 5 * \text{sigmoid}(||p_i - y|| - ||p_a - y||)$ where p_a is the agent position, add penalties to discourage overly short predictions. The $min()$ ensures this component of the loss only provides a reward for improving the better of the two predictions. This allows the network to split the prediction, as there is no penalty for the wrong half of the split. Combined over training data representing ambiguous scenarios, the two predictions are driven towards different, but equally promising next steps.

Simply optimizing the better of two predictions during training is insufficient when one of the two predictions is much further away from the correct node than the other. The second loss term, L_{avg}, addresses this by providing a small penalty for the average of the two predictions:

$$L_{\text{avg}}(p_0, p_1, y) = (||p_0 - y|| + ||p_1 - y||)/2 \quad (3)$$

This term must have a small weight to ensure the primary loss comes from L_{min} to maintain split predictions.

The network also must learn to indicate which of the two predictions is the correct using an output value c. This is accomplished via the third loss term, L_{pred}:

$$L_{\text{pred}}(p_0, p_1, c, y) = |(c - \text{sigmoid}(||p_1 - y|| - ||p_0 - y||)|, \quad (4)$$

where the sigmoid function, $1/(1+e^{-x})$, maps the relative difference between the errors of the two options to the continuous domain $[0, 1]$. This loss will be driven to zero when c matches the (sigmoid of) the relative error. When c is exactly 0 or 1, the agent should move to p_0 or p_1 respectively. When c is between these values, the network can stochastically select an option, leading to a spread of reasonable paths. Unless otherwise stated, for all results we used a k_m of 0.999, a k_a of 0.001, and a k_p of 10.

Figure 3 shows the effect of the network's split prediction. At the top left of the map, the network does not have enough information to know which side of the courtyard is most optimal, and bifurcates the prediction between the two hallways. When the agent is in a less ambiguous part of the building, the network is more confident in the next step. We performed a user study to compare SPNet paths to those taken by real humans for the same tasks (see Appendix E). As Figure 4 shows, in this and other ambiguous scenarios, both user and SPNet paths bifurcate similarly.

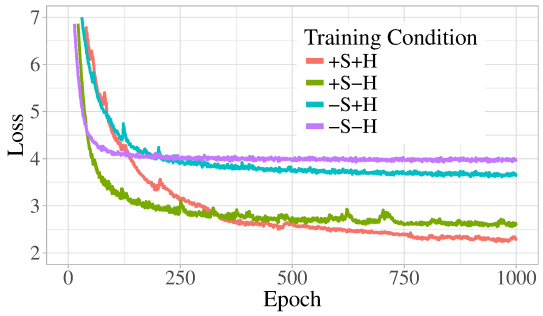

Figure 5: Training Profile Comparisons. A + or − in a condition label denotes presence or absence of an SPNet network feature respectively. "S" and "H" represent split predictions and path history respectively.

4.3 Data Generation & Training

The Scene Representation Network and the Planning Network are trained together as one system. The training data is generated by an exhaustive sampling of every reachable start-goal pair of navigation nodes in training maps (see Appendix D for dataset details). Given a start-goal pair, we permute possible path histories to generate training rows.

In training, the network is never given the actual goal position, but a distribution with a mean sampled from a gaussian centered at the true goal location with uncertainty σ. In order to integrate this uncertain representation into a gradient-based optimization architecture, we employ a custom network layer which samples the fuzzy goal region to generate a specific training instance (the dark shaded box in Figure 1). Importantly, the σ used to perturb the goal location is also an *input to the navigational network*, enabling the input σ to be used as a run-time tuning parameter that controls how much the agent is willing to explore.

The network weights are trained using Keras [Chollet et al. 2015] using stochastic minibatch gradient decent with an ADAM optimizer. Further training details are given in Appendix B.1.

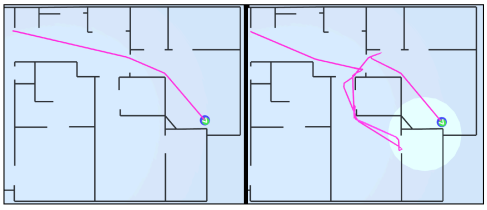

Figure 6: Effect of Goal Uncertainty: The right path has σ = 2.5m and the left has no goal uncertainty. The high uncertainty case produces exploratory behavior as the agent searches for the goal, while the agent on the right heads directly for the certain goal location.

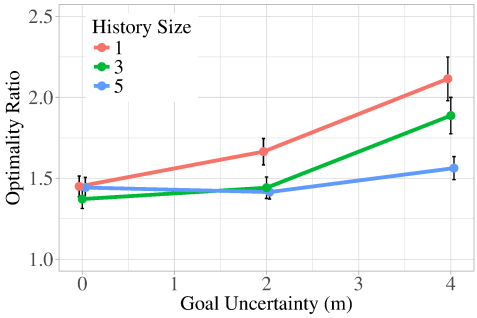

Figure 7: Effect of Behavioral Parameters. Goal uncertainty and history size can be tuned to affect agent behavior. Large uncertainty leads to exploratory behavior, and increasing the history size leads to more optimal paths.

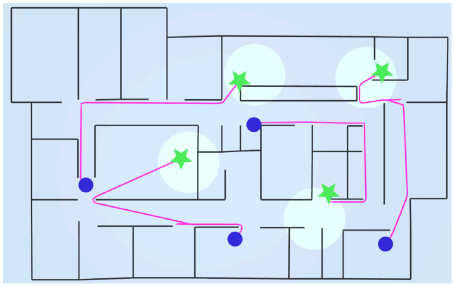

Figure 8: Generalization: Simulated trajectories are shown for an environment not seen in training. Blue dots and green stars indicating the start and goal locations respectively.

5 RESULTS & ANALYSIS

5.1 Network Analysis

As discussed above, allowing the network to split its prediction lead to more human-like behaviors. Additionally, these split predictions improve the training performance of the network. Figure 5 shows a comparison of the SPNet network trained on a single map with 6m of goal uncertainty with and without split predictions. With split predictions enabled, there is over a 60% reduction in the final loss L (from 3.68 down to 2.26). Similarly, the additive representation enabling path history also led to improved loss in training. Figure 5 shows that incorporating path history lead to an additional 15% reduction in the training loss.

5.2 Behavioral Analysis

Our problem formulation and custom network structure allows SPNet agents to display several human-like navigation behaviors that are not possible either with optimal planning techniques or simple local heuristics. SPNet agents respond only to their local conditions, explore in search of vague goals, integrate their observations over time, and intelligently backtrack when they get stuck in local minima. The framework runs in real-time, with a full planning step taking 1-2ms (see Appendix B.2 for runtime details).

As the SPNet predictions are a distribution over two likely possible actions, stochastically selecting one can create a natural diversity of paths. Because the choice of which node to go to next follows the distribution predicted by the network, the agent paths tend to vary more in ambiguous situations (see Figure 4).

Figure 6 shows a SPNet agent navigating past a fork juncture on an apartment-style map. Here, when the goal uncertainty is small (left), the agent navigates straight to the goal, taking a near-optimal path. While this path might be expected from a person who is very familiar with both this building and the exact goal location, its not very reflective of the ambiguity inherent in the navigation task. Increasing the goal uncertainty (right) naturally leads to an exploration behavior.

SPNet agents have two main tunable parameters which can control the behaviors: the size of the goal region σ (creating less certainty in the agents decisions), and the maximum path history n (creating more intelligent backtracking behaviors). These two parameters can also interact with each other. For example, for low σ, paths are more efficient regardless of the size of the path history. When the goal region grows larger, path history becomes more important, especially as the agent needs to reason about which previously explored paths are unlikely to lead to the goal.

Figure 7 explores the interaction of goal uncertainty and path history by comparing SPNet paths to optimal averaged over 200 random tasks spread over the 5 training maps. A larger history size increases path optimality across goal uncertainties, even for history sizes and uncertainties beyond those used in training. A 2-way ANOVA reveals that goal uncertainty has a more significant effect on the agent's path than history (history $F=2.4$, $p < 0.1$, uncertainty $F=7$, $p<0.05$). These results confirm the ability of the scene representation and planning networks to generalize outside the range of parameter values used in training.

Figure 8 (and Appendix C.3) show SPNet agents navigating in a variety of challenging paths on untrained maps. The agents typically find relatively efficient and natural paths that reach their goal despite having never seen the map in training.

6 LIMITATIONS & FUTURE WORK

While SPNet covers an important aspect of a human-like global navigation, it focuses on single agent navigation. Planning in environments with multiple agents typically require specialized search techniques [Atzmon et al. 2020] or hierarchical models [Musse and

Thalmann 2001]. Expanding the network input to include the relative position and velocity of other agents could combine local and global planning into an integrated network. While SPNet is already realtime for a single agent, faster performance may be needed to support large crowd simulations with thousands of agents in a shared scene. Here, it may be possible to accelerate isovist construction using spatial data structures, and to speed up network computation by using GPUs.

In conclusion, we have presented SPNet, a comprehensive framework for human-like global navigation under local information in building environments. The result is a real-time system capable of intelligent navigation behaviors, including exploration and backtracking, environment familiarity, varied routes per task, and efficient but sub-optimal routes toward fuzzy goals.

ACKNOWLEDGMENTS

This work was supported in part by the National Science Foundation under grants IIS-1748541 and CHS-1526693.

REFERENCES

Dor Atzmon, Roni Stern, Ariel Felner, Nathan R Sturtevant, and Sven Koenig. 2020. Probabilistic robust multi-agent path finding. In *Proceedings of the International Conference on Automated Planning and Scheduling*, Vol. 30. 29–37.

Jeremy N Bailenson, Michael S Shum, and David H Uttal. 2000. The initial segment strategy: A heuristic for route selection. *Memory & Cognition* 28, 2 (2000), 306–318.

Somil Bansal, Varun Tolani, Saurabh Gupta, Jitendra Malik, and Claire Tomlin. 2020. Combining optimal control and learning for visual navigation in novel environments. In *Conference on Robot Learning*. 420–429.

Adi Botea, Bruno Bouzy, Michael Buro, Christian Bauckhage, and Dana Nau. 2013. Pathfinding in games. Schloss Dagstuhl-Leibniz-Zentrum fuer Informatik.

Vadim Bulitko. 2004. Learning for adaptive real-time search. *arXiv preprint cs/0407016* (2004).

Vadim Bulitko and Yngvi Björnsson. 2009. kNN LRTA*: Simple Subgoaling for Real-Time Search.. In *AIIDE*.

Lei Cai, Hongyang Gao, and Shuiwang Ji. 2019. Multi-stage variational auto-encoders for coarse-to-fine image generation. In *Proceedings of the 2019 SIAM International Conference on Data Mining*. SIAM, 630–638.

Devendra Singh Chaplot, Dhiraj Gandhi, Saurabh Gupta, Abhinav Gupta, and Ruslan Salakhutdinov. 2020. Learning to explore using active neural slam. *arXiv preprint arXiv:2004.05155* (2020).

Panayiotis Charalambous and Yiorgos Chrysanthou. 2014. The pag crowd: A graph based approach for efficient data-driven crowd simulation. In *Computer Graphics Forum*, Vol. 33. Wiley Online Library, 95–108.

François Chollet et al. 2015. Keras. https://github.com/fchollet/keras.

Carl Doersch. 2016. Tutorial on variational autoencoders. *arXiv preprint arXiv:1606.05908* (2016).

Teófilo Bezerra Dutra, Ricardo Marques, Joaquim B Cavalcante-Neto, Creto Augusto Vidal, and Julien Pettré. 2017. Gradient-based steering for vision-based crowd simulation algorithms. In *Computer graphics forum*, Vol. 36. Wiley Online Library, 337–348.

Russell A Epstein, Eva Zita Patai, Joshua B Julian, and Hugo J Spiers. 2017. The cognitive map in humans: spatial navigation and beyond. *Nature neuroscience* 20, 11 (2017), 1504.

SM Ali Eslami, Danilo Jimenez Rezende, Frederic Besse, Fabio Viola, Ari S Morcos, Marta Garnelo, Avraham Ruderman, Andrei A Rusu, Ivo Danihelka, Karol Gregor, et al. 2018. Neural scene representation and rendering. *Science* 360, 6394 (2018), 1204–1210.

Saurabh Gupta, James Davidson, Sergey Levine, Rahul Sukthankar, and Jitendra Malik. 2017. Cognitive mapping and planning for visual navigation. In *Proceedings of the IEEE Conference on Computer Vision and Pattern Recognition*. 2616–2625.

Carlos Hernández and Pedro Meseguer. 2005. LRTA*(k). In *Proceedings of the 19th international joint conference on Artificial intelligence*. 1238–1243.

Marcelo Kallmann and Mubbasir Kapadia. 2014. Navigation meshes and real-time dynamic planning for virtual worlds. In *ACM SIGGRAPH 2014 Courses*. 1–81.

Mubbasir Kapadia, Nuria Pelechano, Jan Allbeck, and Norm Badler. 2015. Virtual crowds: Steps toward behavioral realism. *Synthesis lectures on visual computing: computer graphics, animation, computational photography, and imaging* 7, 4 (2015), 1–270.

Raphael Kaplan, Nicolas W Schuck, and Christian F Doeller. 2017. The role of mental maps in decision-making. *Trends in Neurosciences* 40, 5 (2017), 256–259.

Ioannis Karamouzas, Brian Skinner, and Stephen J Guy. 2014. Universal power law governing pedestrian interactions. *Physical review letters* 113, 23 (2014), 238701.

Ioannis Karamouzas, Nick Sohre, Rahul Narain, and Stephen J Guy. 2017. Implicit crowds: Optimization integrator for robust crowd simulation. *ACM Transactions on Graphics (TOG)* 36, 4 (2017), 1–13.

Sven Koenig and Maxim Likhachev. 2002. D^* lite. *Aaai/iaai* 15 (2002).

Sven Koenig and Xiaoxun Sun. 2009. Comparing real-time and incremental heuristic search for real-time situated agents. *Autonomous Agents and Multi-Agent Systems* 18, 3 (2009), 313–341.

Richard E Korf. 1990. Real-time heuristic search. *Artificial intelligence* 42, 2-3 (1990), 189–211.

Steven M LaValle. 1998. Rapidly-exploring random trees: A new tool for path planning. (1998).

Seunghwan Lee, Moonseok Park, Kyoungmin Lee, and Jehee Lee. 2019. Scalable muscle-actuated human simulation and control. *ACM Transactions on Graphics (TOG)* 38, 4 (2019), 1–13.

William Lee and Ramon Lawrence. 2013. Fast grid-based path finding for video games. In *Canadian Conference on Artificial Intelligence*. Springer, 100–111.

Antonio Lima, Rade Stanojevic, Dina Papagiannaki, Pablo Rodriguez, and Marta C González. 2016. Understanding individual routing behaviour. *Journal of The Royal Society Interface* 13, 116 (2016), 20160021.

Pinxin Long, Tingxiang Fanl, Xinyi Liao, Wenxi Liu, Hao Zhang, and Jia Pan. 2018. Towards optimally decentralized multi-robot collision avoidance via deep reinforcement learning. In *2018 IEEE International Conference on Robotics and Automation (ICRA)*. IEEE, 6252–6259.

Tomás Lozano-Pérez and Michael A Wesley. 1979. An algorithm for planning collision-free paths among polyhedral obstacles. *Commun. ACM* 22, 10 (1979), 560–570.

Ying-Sheng Luo, Jonathan Hans Soeseno, Trista Pei-Chun Chen, and Wei-Chao Chen. 2020. CARL: Controllable Agent with Reinforcement Learning for Quadruped Locomotion. *ACM Trans. Graph.* 39, 4, Article 38 (July 2020), 10 pages. https://doi.org/10.1145/3386569.3392433

Rachel McDonnell, Michéal Larkin, Simon Dobbyn, Steven Collins, and Carol O'Sullivan. 2008. Clone attack! perception of crowd variety. In *ACM SIGGRAPH 2008 papers*. 1–8.

Soraia Raupp Musse and Daniel Thalmann. 2001. Hierarchical model for real time simulation of virtual human crowds. *IEEE Transactions on Visualization and Computer Graphics* 7, 2 (2001), 152–164.

Jan Ondřej, Julien Pettré, Anne-Hélène Olivier, and Stéphane Donikian. 2010. A synthetic-vision based steering approach for crowd simulation. *ACM Transactions on Graphics (TOG)* 29, 4 (2010), 1–9.

C. Peters and C. O'Sullivan. 2002. Synthetic Vision and Memory for Autonomous Virtual Humans. *Computer Graphics Forum* 21, 4 (2002), 743–752. https://doi.org/10.1111/1467-8659.00632 arXiv:https://onlinelibrary.wiley.com/doi/pdf/10.1111/1467-8659.00632

Mark Pfeiffer, Michael Schaeuble, Juan Nieto, Roland Siegwart, and Cesar Cadena. 2017. From perception to decision: A data-driven approach to end-to-end motion planning for autonomous ground robots. In *2017 ieee international conference on robotics and automation (icra)*. IEEE, 1527–1533.

Mark Pfeiffer, Samarth Shukla, Matteo Turchetta, Cesar Cadena, Andreas Krause, Roland Siegwart, and Juan Nieto. 2018. Reinforced imitation: Sample efficient deep reinforcement learning for mapless navigation by leveraging prior demonstrations. *IEEE Robotics and Automation Letters* 3, 4 (2018), 4423–4430.

Sadegh Rabiee and Joydeep Biswas. 2019. IVOA: Introspective Vision for Obstacle Avoidance. In *Intelligent Robots and Systems (IROS), IEEE/RSJ International Conference on*. IEEE. https://joydeepb.com/Publications/iros2019_ivoa.pdf

Nathan R Sturtevant and Vadim Bulitko. 2011. Learning where you are going and from whence you came: h-and g-cost learning in real-time heuristic search. In *IJCAI*. Citeseer, 365–370.

Vivienne Sze, Yu-Hsin Chen, Tien-Ju Yang, and Joel S Emer. 2017. Efficient processing of deep neural networks: A tutorial and survey. *Proc. IEEE* 105, 12 (2017), 2295–2329.

Aviv Tamar, Yi Wu, Garrett Thomas, Sergey Levine, and Pieter Abbeel. 2016. Value iteration networks. In *Advances in Neural Information Processing Systems*. 2154–2162.

Jur van den Berg, Ming Lin, and Dinesh Manocha. 2008. Reciprocal velocity obstacles for real-time multi-agent navigation. In *2008 IEEE International Conference on Robotics and Automation*. IEEE, 1928–1935.

Wouter van Toll, Roy Triesscheijn, Marcelo Kallmann, Ramon Oliva, Nuria Pelechano, Julien Pettré, and Roland Geraerts. 2016. A comparative study of navigation meshes. In *Proceedings of the 9th International Conference on Motion in Games*. 91–100.

He Wang, Jan Ondřej, and Carol O'Sullivan. 2016. Path patterns: Analyzing and comparing real and simulated crowds. In *Proceedings of the 20th ACM SIGGRAPH Symposium on Interactive 3D Graphics and Games*. 49–57.

A EXECUTION DETAILS

Algorithms 1 & 2 detail the SPNet execution strategy. Because SPNet executes very quickly, it is possible to plan fully to the goal and smooth away minor inefficiencies in the resulting path. Here, we generally avoid such smoothing techniques as they can suppress desired exploration behaviors. One exception is that if a network predicts visiting a node it has already visited (or a node for which the agent has already seen all of the node's neighbors), the we allow the agent to move directly toward the next predicted node as soon as it comes into view. In practice, the particular character animation system used may provide some additional path smoothing as the character animates between nodes.

Algorithm 1: SPNet

```
Input: map (Walls and Nodes), start (Node), goal (Node),
  goalRegionMean (Position), goalRegionSigma (float)
Output: path (Node List)
#global maxVisitCount = 3;
/* visit count for each node                                  */
#global visits = [0] * map.numNodes;
/* path is full route (will include back-tracking sequences) */
path = [];
/* history is path with cycles removed                        */
history = [];
current = start;
while current != goal do
    next = SPNetStep(map,current,goalRegionMean,
      goalRegionSigma,history,path);
    path.push(next);
    current = next;
end
return path;
```

Algorithm 2: SPNet Step

```
Input: map (Walls and Nodes), current (Node), goal(Node),
  goalRegionMean (Position), goalRegionSigma (float),
  history (Node List), path (Node List)
Output: next (Node) visits[current]++;
if isVisible(goal) then
    next = goal;
else
    /* gets all visible nodes from current node visited less
       than maxVisitCount times                                */
    candidates = map.getVisibleNodes(current,
      maxVisitCount);
    if candidates.size == 0 then
        /* retrace our steps                                  */
        next = history.pop();
    else
        position = getNetworkPrediction(current,
          goalRegionMean, goalRegionSigma, candidates,
          path);
        next = map.getClosestNode(position);
        history.push(current);
    end
end
return next;
```

B NETWORK DETAILS

B.1 Training Details

The network was trained on 10 cores of an 2.3 GHz Intel(R) Xeon(R) CPU. Training was run for 230 epochs that iterated through all the training data, with each epoch taking about 3 minutes, and the entire run taking 12 hours. As can be seen in Figure 9, most of the improvements in loss came at the start of training, but the longer run ensured the network had sufficient time to converge.

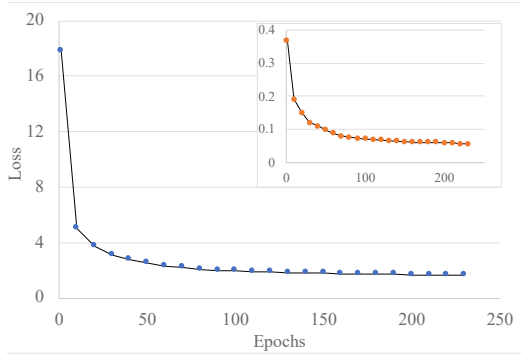

Figure 9: Training Loss: Total training loss (outset) and just the predictions loss L_{pred} (inset) throughout training.

Training was performed across 5 maps and included all possible paths with a history of length three for a total of 2,315,665 training examples, each of which was sampled with three levels of goal uncertainty (sampled from 0, 1, and 2m gaussian distributions respectively), leading to about 7 million samples trained each epoch. Epochs were trained in batches of size 100,000 using the Keras framework with the ADAM optimizer and a dynamic learning rate that started at 3e-4 and ended at 1e-5.

To improve numerical stability, isovist ray lengths are normalized to lie on the interval $[0, 3]$ by dividing by 1/3 of the maximum length of 30m. Unless otherwise stated below, the network was trained with a goal uncertainty $\sigma \in \{0, 1, 2\}$ meters, and a maximum path history of size 3. We note that while 2m may seem like a small distance, in practice sampling from a 2D gaussian with i.i.d dimensions at $\sigma = 2m$ often yields points significantly farther than 2m from the mean (in fact, the 1 std dev circle having diameter 4m will probabalistically contain less than half of sampled points). As discussed in Section 5.2, the network was able to extrapolate good behavioral performance beyond the uncertainties and history sizes on which it was trained.

B.2 Runtime Breakdown

The runtime of SPNet planning is dominated by three major components. Figure 10 shows the runtime breakdown of each for maps of various sizes. All experiments were run on a desktop PC with an Intel i7 4770K CPU and 16GB of memory. While computing

Table 1: User study and participant summary.

	Users	Tasks		Avg. Samples/Task	Game Experience (hrs/mo)			
		Trained	Untrained		None/Rare	1-4	5-20	20+
Study 1 (selected tasks)	48	8	2	40.45	13	11	9	15
Study 2 (random tasks)	27	25	15	9.85	7	5	9	6

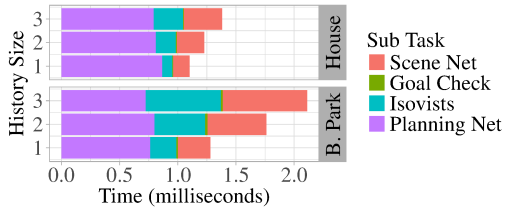

Figure 10: SPNet Runtime: Average total runtime for each step of planning in SPNet across history and map size. 50 random tasks were executed for a small (House) and large (Business Park) map to generate timing samples. Runtime cost is primarily split between executing the prediction network, scene network, and computing isovist features.

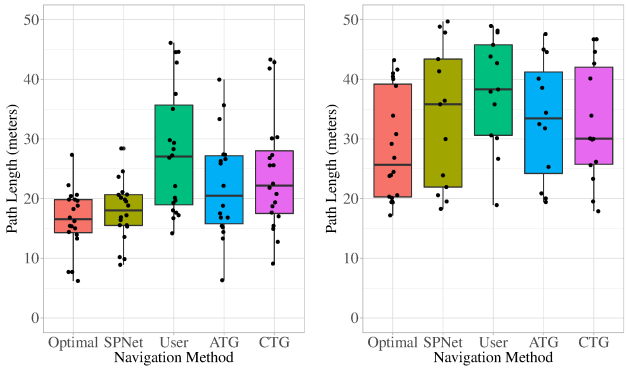

(a) Trained Maps **(b) Untrained Maps**

Figure 11: Differences from mean user path lengths on Round 2 of the User study for trained and untrained map sets.

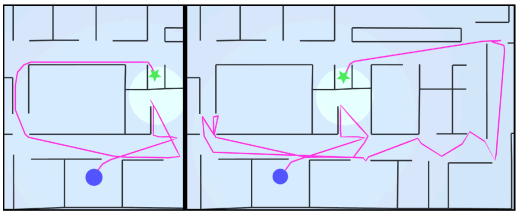

Figure 12: Effect of Path History: Two simulated trajectories for the same task. The left path was generated by an agent with no path history, and the right trajectory the agent incorporates the past three visited map nodes in planning.

isovists takes longer on larger maps as more visibility checks are needed, the planning network runtimes are fairly constant. Longer path histories add incremental cost as the scene representation network is run once per recalled isovist. Even for very large maps, SPNet runs in realtime, taking less than 2ms to output a next step. If faster performance is required, isovists can be precomputed for each navigation node.

C FURTHER BEHAVIORAL ANALYSIS

C.1 Comparison to Local Heuristics

SPNets bridge the gap between global planning techniques and local navigation heuristics. Human route selection studies have revealed high-quality local route selection heuristics that strongly influence human paths. Two of these techniques from the cognitive science domain that can be directly implemented in the broader navigation framework of this paper are:

- Traveling as far as possible towards a goal [Bailenson et al. 2000], which we will refer to as Closest-to-Goal (CTG)
- Maintaining a small relative angle in heading with respect to the goal [Lima et al. 2016], which we will refer to as Angle-to-Goal (ATG)

Figure 11 shows the results of replacing the network predictions with CTG and ATG-based heuristics. When compared to the tasks in the user study data (see Appendix E), both CTG and ATG had path lengths which were more similar to human paths that the optimal route selection. This result is consistent with the existing findings in psychology of the general importance and applicability of these local navigation heuristics to humans. On the tasks tested in the user study, SPNet matches human path lengths as well as (or better than) these heuristics, while exhibiting more natural behaviors (ATG tends to oscillate and CTG can get stuck in obstacle local minima) and supporting uncertain goals and memory integration.

Some over-fitting effects can be observed in trained maps where SPNet produces path lengths closer to optimal than human paths, while matching human path lengths better on untrained maps. This suggests that techniques to help combat over-fitting such as larger training data sets and early-stopping may further improve SPNet's path quality on trained maps. Alternatively, this over-fitting can be exploited as a feature when agents should exhibit familiarity with a particular environment.

C.2 Effect of History

Figure 12 shows an example of the key navigational behaviors SPNet agents exhibit. On the left is an agent with a max path

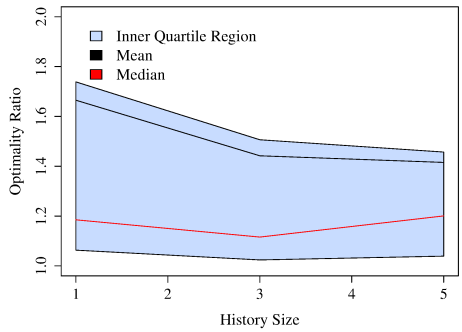

Figure 13: Effect of history size on path optimally averaged across all paths with goal size σ=2.

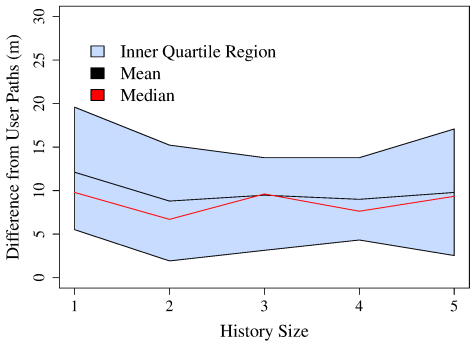

Figure 14: Remembering the Past: Our representation network allows for the integration of past observations that influences future decisions, resulting in more human-like path lengths on untrained maps.

history of 3 isovists and a relatively large goal distribution (σ = 2m of uncertainty, shown as the shaded circle at 1 std dev radius). After initially exploring the room overlapping the bottom half of the goal distribution, the agent rules out the area as a potential goal location and remembers this as it travels up the left side of the environment. In contrast, an agent who is using only its single, current isovist (no path history) is unable to remember where it has been. Figure 12 right shows such an agent, who must return to places it had been before, eventually finding a longer route to the goal.

We can effectively increase the size of the history simply by summing additional encodings together before sending them to the planning network. As shown in Figure 7 and Figure 14, this additive encoding scheme allows the SPNet to make meaningful use of additional history even outside the sizes it was trained on. Figure 13 shows the effect of planning over longer histories on the optimality of the resulting paths. Plans that account for more history lead to more optimal paths, even when using longer histories than were seen in training.

Table 2: Datasets: the collection of maps analyzed in this work. The table indicates the size of the maps, and the number of instances of training data that would be generated from that map. The three largest maps and one smaller map were excluded from training and used to test generalization.

	Walls	Nodes	Size (m)	Data (#)	Use
Simple	29	28	12x8	16 K	Train
Apartment	65	65	14x9	157 K	Train
House	72	84	29x19	168 K	Train
Courtyard	75	97	17x12	867 K	Train
Medical	101	109	23x27	1.1 M	Train
Office	84	95	28x17	781 K	Test
University Labs	129	154	44x26	4.66 M	Test
Business Park	161	197	33x27	4.60 M	Test
Conference	276	332	61x33	15.44 M	Test

C.3 Generalizing to Large Maps

SPNet agents can perform well on large maps not seen in training even for relatively long or complex tasks (Figures 16, 15).

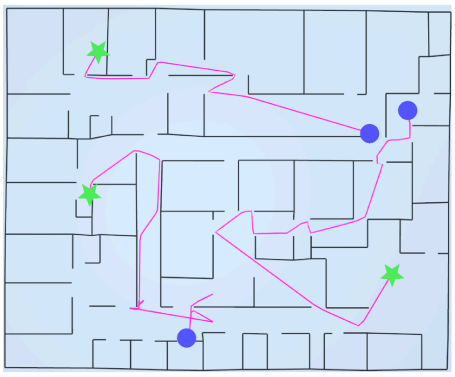

Figure 15: Selected SPNet trajectories on a business suites map (history size 3, uncertainty = 0m).

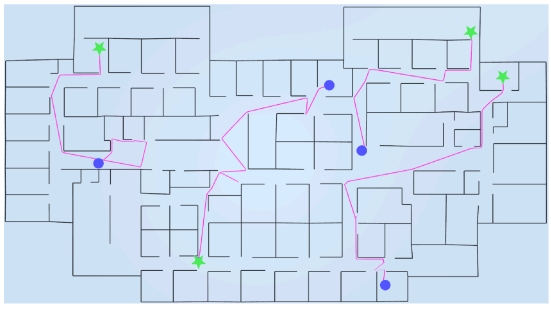

Figure 16: Selected SPNet trajectories on a conference center map (history size 3, uncertainty = 0m).

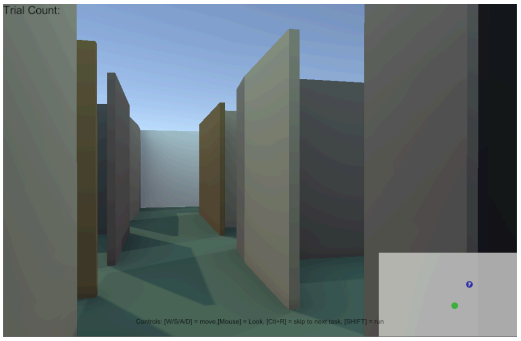

Figure 17: User Study: Snapshot from the user-study tasks. Participants were asked to navigate to a goal whose relative position was indicated by by the green dot in the minimap in the lower right.

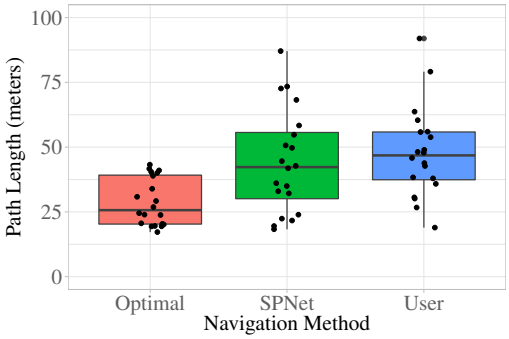

Figure 18: Path Length Comparison: Human users take longer paths than the graph-optimal sequence. For trained maps, SPNet path lengths are close to graph-optimal, but on new maps SPNet paths are closer to the paths taken by humans.

D DATASETS

While we employ a supervised learning approach, it would be impractical to gather enough human trajectory data to demonstrate good behavior on a meaningful percentage of the potential tasks. For example, the 6 maps we use in our training dataset contain 6.9 million training examples of different start goal pairs permuted with possible previous observations. In order to create this data, we instead use a graph-optimal search to determine the optimal path from start to goal, and use the resulting step-wise decisions in training.

While the SPNet network is trained on optimal paths, our goal is not to produce purely optimal behavior. Rather, attempting to be globally optimal while restricting the network to only local, uncertain information results in paths with human-like sub-optimal behaviors, even on maps used in training.

To facilitate training and evaluation, we create a dataset of environments based on real floor plans from a variety of buildings of different shapes and sizes (see Figures 19 and 20). Maps used in training the network include three smaller buildings, two larger buildings, and a small test map made by hand. This dataset consists of a wide range of different environments, with very different types of layouts, and very different sizes (see Table 2). Additionally, we withheld a set of maps from training to be used in analysis of how the method performs in untrained scenarios. All maps are rendered in Figures 20 and 19.

E USER STUDY

To validate the human-like properties of SPNet paths, we gathered human paths via a user study approved by the Institutional Review Board (IRB). During the the study, participants performed navigation tasks via a 3D game-like interface in a web browser (on their own machines) through a rendering of the maps in Table 2. A minimap displayed a live update of the relative goal location, but not walls in order to provide some natural uncertainty in the exact goal location (see Figure 17). Participants were asked to aim to complete 15 navigation tasks, but were allowed to do as many or few as they chose, with the average user completing 16.9 navigation tasks (see Table 1 for additional details). Each user was given a sample "warm-up" task to acclimate to the controls. As the user moved through each task, their trajectory was tracked at a frequency of 10 samples per meter displacement. Trajectories for the same tasks were generated using SPNet, with the goal region centered on the true goal position. Before performing analyses, both user and simulated paths are put through a low-pass running median filter as implemented in the *runmed* function of the R statistical programming language with k=11 to remove any small jittering in the paths. Users took one of two versions of the study: the first consisted of randomized hand-picked tasks for qualitative comparison (879 trajectories captured), and the second consisted of random tasks across all maps for quantitative comparisons (394 trajectories captured).

Quantitatively, we see SPNet has more similar path lengths to humans than graph-optimal planning. Figure 18 shows that path lengths of SPNet agents are more similar to study participants than paths generated using the graph-optimal routing. An ANOVA with Tukey post-hoc analysis shows strong separation between optimal path lengths and user path lengths as well as SPNet path lengths ($p < 0.05$), while showing the User and SPNet distributions as similar (p 0.43). Qualitatively, the user study results show SPNet captures the natural, efficient, and varied paths real humans take. Figure 4(left) shows SPNet on an ambiguous task in the Courtyard map, which was included in training. Here, SPNet agents follow different paths that encompass the majority of the types taken by the users in the study. In a similarly ambiguous task on the untrained University Labs map, Figure 4(right), SPNet agents are capable of finding both homotopies portrayed in human routes. In practice, we find SPNet agents tend to produce compelling split predictions in untrained environments, but are overly confident between the two choices as compared to maps seen in training. Therefore, while SPNet agents show exploration behaviors, and human-like path lengths in both trained and untrained maps, it may be best in practice to train on maps when possible to ensure more path variety.

Below we show the maps used in training (Figure 19) and testing (Figure 20). All environments were based on real floor plans, abstracting away irrelevant obstacle detail.

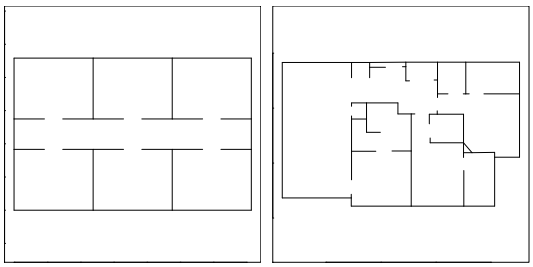

(a) Simple (b) Apartment

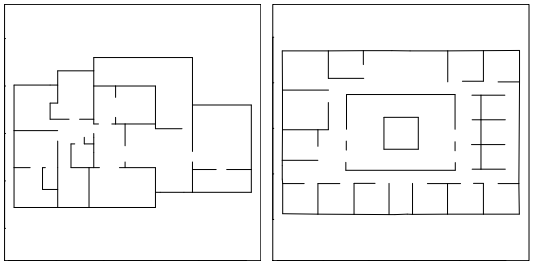

(c) House (d) Courtyard

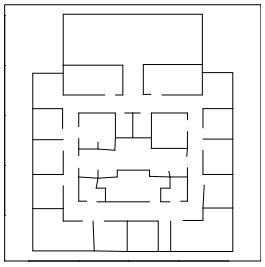

(e) Medical

Figure 19: Training Maps.

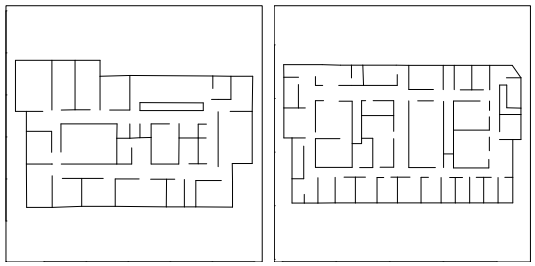

(a) Office (b) University Labs

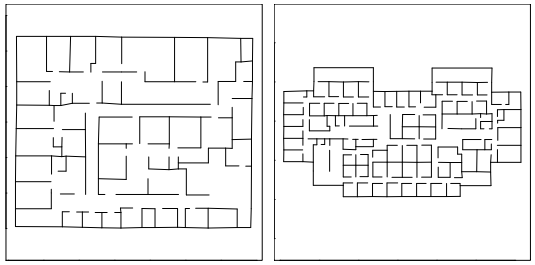

(c) Business Park (d) Conference

Figure 20: Testing Maps.